

C-axis Electronic Raman Scattering in $\text{Bi}_2\text{Sr}_2\text{CaCu}_2\text{O}_{8+\delta}$

H.L. Liu,¹ G. Blumberg,¹ M.V. Klein,¹ P. Guptasarma,² and D.G. Hinks²

¹ *Department of Physics and Science and Technology Center for Superconductivity,
University of Illinois at Urbana-Champaign, Urbana, Illinois 61801-3080*

² *Materials Science Division and Science and Technology Center for Superconductivity,
Argonne National Laboratory, Argonne, Illinois 60439*

(March 11, 2018)

Abstract

We report a *c*-axis-polarized electronic Raman scattering study of $\text{Bi}_2\text{Sr}_2\text{CaCu}_2\text{O}_{8+\delta}$ single crystals. In the normal state, a resonant electronic continuum extends to 1.5 eV and gains significant intensity as the incoming photon energy increases. In the superconducting state, a coherence 2Δ peak appears around 50 meV, with a suppression of the scattering intensity at frequencies below the peak position. The peak energy, which is higher than that seen with in-plane polarizations, signifies distinctly different dynamics of quasiparticle excitations created with out-of-plane polarization.

PACS numbers: 74.72.Hs, 78.20.-e, 78.30.-j

One of the peculiar aspects of the high- T_c cuprates is the incoherent nature of the charge transport perpendicular to the CuO_2 planes [1]. Early on it was established experimentally that the normal-state in-plane resistivity typically varies linearly with temperature, whereas the out-of-plane resistivity almost universally displays semiconducting behavior [2]. The c -axis optical conductivity of the most cuprates [3,4] shows an electronic background with a very large scattering rate – that is the mean free path appears to be less than the lattice spacing. These results suggest that there is no coherent electronic transport in the c -direction: all motions are inelastic. A number of models have been proposed to explain the important mechanisms contributing to c -axis transport in high- T_c superconductors, including localization along the c -axis [5], carrier confinement in the resonating valence bond (RVB) theory [6], and interlayer tunneling (ILT) or hopping [7,8]. However, there is currently no consensus as to the clear picture of the origin of incoherent c -axis transport.

Among all cuprate superconductors, the double-layered $\text{Bi}_2\text{Sr}_2\text{CaCu}_2\text{O}_{8+\delta}$ (Bi-2212) crystal is the most decoupled material. In Bi-2212, the ratio of the out-of-plane to in-plane resistivity ρ_c/ρ_{ab} can be as high as 10^5 [9]. Optical response shows that the c -axis reflectivity of Bi-2212 is highly insulating, while the in-plane reflectivity is metallic [3]. The corresponding plasma frequency anisotropy in Bi-2212, $\omega_{pab}/\omega_{pc} > 100$, is substantially larger than that observed in other cuprates. These data provide evidence that the c -axis transport of Bi-2212 is incoherent, with the extremely small energy scale set by the hopping interaction between the adjacent CuO_2 bilayers. In the superconducting state, the two-dimensional character of Bi-2212 also manifests itself strongly in the penetration depth measurements. The c -axis penetration depth is extremely large ($\lambda_c \approx 100 \mu\text{m}$) [10]. The large anisotropy between λ_{ab} and λ_c of Bi-2212 was shown to be best described within a picture of strongly superconducting CuO_2 layers weakly coupled by Josephson interaction along the c -axis [11].

The purpose of this study is to investigate, in the context of electronic Raman scattering spectroscopy, the role of c -axis polarizability in the Bi-2212 cuprates. Raman scattering has been proved to be a valuable technique for understanding the quasiparticle dynamics on different regions of the Fermi surface in the cuprate systems by orienting incoming and

outgoing photon polarizations [12]. The electronic Raman spectra polarized in the ab -plane of Bi-2212 have been extensively studied [13]. In contrast, Raman data on the electronic scattering of Bi-2212 for photons polarized along the c -axis are rare [14]. Our new results show that the electronic continuum in zz -polarization does exist and is not small. Notably, this continuum intensity resonates towards near ultraviolet (UV) photon excitation. Below T_c , there is a measurable superconductivity-induced redistribution of the zz -polarized continuum and the presence of a 2Δ peak-like feature, similar to those observed in the ab -plane Raman response.

Single crystals of Bi-2212 were grown near-stoichiometric using a solvent-free Floating Zone process in a double-mirror image furnace modified for very slow growth. In this letter, we used an as-grown, un-annealed single crystal of dimensions $5 \times 1 \times 0.5 \text{ mm}^3$ with a superconducting transition onset at 87 K (dc magnetization) and onset-to-saturation midpoint at 85 K. The Raman measurements were performed on two faces of the crystal. One face (labeled I in Fig. 1) contains both the c -axis and either the a - or b - direction. The second face, face II, provided the a - and b -axis response. We have also studied another sample ($T_c = 93 \text{ K}$, $\Delta T_c = 1.5 \text{ K}$) with less surface quality of face I and obtained similar results. Throughout this study, x and y are indexed along the Bi-O bonds, rotated by 45° with respect to the Cu-O bonds. All symmetries refer to a tetragonal D_{4h} point group.

The low-frequency Raman spectra were taken in pseudobackscattering geometry with $\hbar\omega_i = 1.92 \text{ eV}$ photons from a Kr^+ laser. The laser excitation of less than 10 W/cm^2 was focused into a $50 \mu\text{m}$ diameter spot on the sample surface. The temperatures referred to in this paper are the nominal temperatures inside the cryostat. The spectra were analyzed by a triple grating spectrometer with a liquid-nitrogen cooled charge-coupled device detector. To investigate further the resonance property, we have used several excitation lines from Ar^+ and Kr^+ lasers ranging from visible red to near UV. All the Raman spectra were corrected for the spectral response of the spectrometer and detector, the optical absorption of the sample as well as the refraction at the sample-gas interface [15].

The imaginary parts of the c -axis-polarized Raman response functions, obtained by di-

viding the original spectra by the Bose-Einstein thermal factor, are shown in Fig. 1 for two different temperatures, 100 K ($T > T_c$) and 5 K ($T \ll T_c$). In the normal state, the most prominent features of the spectra are the electronic continuum and several $q \approx 0$ Raman allowed phonon modes, whose overall character is in good agreement with that reported previously [16–18]. We focus on the temperature behavior of the electronic Raman scattering response. Well below T_c , it can be seen in Fig. 1 that for the zz continuum there is a loss of scattering strength at low frequencies which redistributes into the weak and broad peak at higher frequencies. Above 700 cm^{-1} , the 5 K and 100 K spectra appear to be essentially identical. These data were reproducibly observed at three different spots on the sample. We emphasize that the redistribution of the scattering intensity itself is not of phononic origin. The low energy (red) excitation is used primarily to reduce the intensity of phononic scattering. Furthermore, a similar feature has been reported for other less anisotropic members of the high- T_c superconductors, including $\text{YBa}_2\text{Cu}_3\text{O}_{7-\delta}$ (YBCO) [19] and $\text{NdBa}_2\text{Cu}_3\text{O}_{7-\delta}$ [20].

In order to observe the superconductivity-induced redistribution of the electronic continuum better, in the inset of Fig. 1 we present the change between the normal and superconducting spectra in an enhanced manner, where the 5 K spectrum is normalized by (1) dividing by the 100 K spectrum (top curve), (2) subtracting the 100 K spectrum (middle curve), and (3) the difference of Raman spectra, as in (2), after first subtracting the phonon contributions (bottom curve). We believe that sharp features in difference spectra are due to temperature dependence of phononic scatterings. It is nevertheless clear that in all cases below T_c a broad peak forms in the electronic continuum which is accompanied by reduced scattering at the lowest Raman shift. The difference vanishes at sufficiently high frequencies.

It is instructive to compare the c -axis electronic continuum with results for other scattering configurations, which are shown in Fig. 2. As can be seen in the Fig. 2(a), a depolarized zx spectrum has an even smaller continuum intensity compared with that from the zz component. Furthermore, the normal and superconducting spectra are indistinguishable. In contrast, the superconducting transition leads to the redistribution of the continuum into

a broad peak in xx polarization (Fig. 2(b)). It is interesting to note that the out-of-plane and in-plane xx spectra (Fig. 2(c)) look almost identical. We have also found that there is an x - y anisotropy clearly demonstrated by the phonon modes between in-plane xx and yy (Fig. 2(f)) polarizations [17]. Referring to the Fig. 2(e), the B_{1g} contribution is predominant in xy geometry, and gives an electronic continuum that is much stronger than that in any other polarization. Below T_c , the strong suppression of the continuum is observed, and the low-frequency intensity varies roughly as ω^3 , while it is quite linear in $x'y'$ (Fig. 2(d)) polarization ($B_{2g} + A_{2g}$ symmetry). At the same time, the magnitude of superconductivity-induced peak is much less intense in $B_{2g} + A_{2g}$ symmetry than that found in B_{1g} symmetry. Such ω dependences in both scattering geometries are consistent with an order parameter of d -wave symmetry [$d(x^2 - y^2)$ when referred to Cu-O bonds] [21].

The results presented in Figs. 1 and 2 clearly show that the intensity of the c -polarized continuum is not negligible compared with that of the in-plane symmetries. We regard these observations as truly extraordinary, for c -axis transport is incoherent. To examine what microscopic origins might produce the zz continuum in Bi-2212, we first discuss our data in terms of the conventional model of light scattering from a superconductor [21,22]. In this model, the strength of the electronic Raman scattering is proportional to the square of the Raman vertex. For nonresonant excitation, the Raman vertex at a point k in reciprocal space is given approximately by the inverse effective mass (the curvature of the energy band dispersion), $\gamma_{ij} \propto \frac{1}{m_{ij}^*} \propto \frac{\partial^2 \epsilon(k)}{\partial k_i \partial k_j}$. In Bi-2212, both transport [3,9] and band structure calculations [23] reflect the fact that the c -axis effective mass is in general very heavy. Consequently, the c -axis nonresonant Raman scattering should be truly small. We see, instead, an ordinary size for the electronic Raman scattering intensity along the c -direction, and suggest that this is a result of a resonance Raman vertex.

To illustrate this consideration, we show in Fig. 3 on an expanded scale room-temperature c -axis Raman spectra excited with photon energies between 1.92 and 3.05 eV. For the latter incident energy, we followed the continuum to 1.5 eV Raman shift. The continuum intensity exhibits a dramatic increase when the excitation approaches the UV region. This

is more clearly seen in the inset of Fig. 3 where we plot the resonance profile for the zz - and xx -polarized continua. The continuum intensity was measured at around 2000 cm^{-1} and normalized to its value at 3.05 eV . We note that the zz continuum gains intensity by a factor of ≈ 5 towards UV excitation, while the change of the xx continuum intensity is rather modest. Due to the limited number of data points, especially below 2 eV , it is difficult to discriminate between nonresonance and resonance Raman vertex contributions to the scattering intensity. However, the substantially different resonance behavior of the zz and xx continua is in qualitative agreement with what one might expect from the strong anisotropy of the frequency-dependent Raman vertex [24], which can be interpreted as an inverse frequency-dependent effective mass: If one were to extrapolate the resonance data to zero frequency, the value of the out-of-plane continuum scattering efficiency would be close to zero and significantly smaller than that of the in-plane symmetry. This is consistent with a great anisotropy in the carrier effective mass, and supported by the transport and band structure studies – that is $m_{ab}^*(\omega = 0) \ll m_c^*(\omega = 0)$.

From Fig. 3, the pronounced resonance effect on the zz continuum follows approximately the trend of the imaginary part of the c -axis dielectric constant [3,25], indicating that light couples to the c -axis continuum *via* some intermediate excitation states with energy $> 3\text{ eV}$. We believe that the scattering process in zz geometry is mediated by transitions occurring between the CuO_2 and Bi-O layers. This view is further supported by the band theories of Bi-2212 showing that two $\text{Bi-O}(3)$ bands lie mostly $2\text{-}3\text{ eV}$ above the Fermi energy E_F along the $\Gamma - Z$ direction [23]. The earlier c -axis Raman scattering studies of YBCO indicated that the resonance behavior results from the modulation of an optical transition between CuO_2 plane band and chain band [26]. More recently, a theoretical study of the c -axis normal-state Raman scattering also suggested that in some cases the contribution of interband transitions dominate the Raman response [27].

We now discuss the c -axis electronic Raman scattering response in the superconducting state. As shown in Figs. 1 and 2, a broad peak in the c -axis continuum developed below T_c is similar to the data (so-called coherent “ 2Δ peak”) observed in the ab -plane. However, there

are some differences between the spectra as well. The peak position in zz occurs near 400 cm^{-1} (50 meV). This feature, which has A_{1g} symmetry, is found at higher frequency than that seen in the planar B_{1g} (360 cm^{-1}), B_{2g} (345 cm^{-1}), and A_{1g} (300 cm^{-1}) symmetries, but it has a smaller intensity than its in-plane counterparts. It is worth mentioning that the B_{1g} peak energy gives $2\Delta/k_B T_c$ a value of 6.1, similar to that reported in prior work on overdoped Bi-2212 [13]. We are presently unaware of any theoretical work that would describe the c -axis Raman response at $T < T_c$. It is unclear why the energy scale of the 2Δ peak associated with the out-of-plane and the A_{1g} part of the in-plane response is different. We can say with some certainty that the Raman scattering process in both cases creates two quasiparticles. We do not know whether or not they are on the same CuO_2 plane. Perhaps the difference between the two spectra of A_{1g} symmetry occurs because they contain different admixtures of same-plane and different-plane pairs of quasiparticles. The two kinds of pairs could be expected to undergo distinct final state interactions and screening corrections. The c -axis Raman measurements on single-layer $\text{Bi}_2\text{Sr}_2\text{CuO}_6$ would augment this study nicely.

Finally, it is of interest to compare our Raman data with the recent measurements of the c -axis microwave conductivity $\sigma_{1c}(T)$ [28]. In optimally doped Bi-2212, $\sigma_{1c}(T)$ falls rapidly below T_c , with no sign of the broad maximum observed in the ab -plane [29]. The behavior of $\sigma_{1c}(T)$ shows that the c -axis transport remains incoherent down to the superconducting transition, and below T_c is better approached as a case of the Josephson tunneling [30]. The existence of well-defined “ 2Δ peak” in our Raman results suggests that three-dimensional superconducting coherence is present in overdoped Bi-2212 at low temperatures below T_c .

In summary, c -axis electronic Raman scattering spectra have been investigated for Bi-2212 single crystals. Our most significant result is the observation of the c -axis electronic continuum up to very high energies, even though the transport in the c -direction is incoherent. The continuum intensity dramatically increases using UV photon excitation, suggesting that the scattering process in zz geometry is dominated by a resonance Raman vertex. Below T_c , there is a clear low-energy redistribution of the continuum. The appearance of a 2Δ peak is a signature of three-dimensional superconducting coherence. Moreover, the greater

value of the peak energy, relative to the in-plane cases, signifies that different quasiparticle dynamics are involved.

We thank S.L. Cooper, K.E. Gray, and A.J. Leggett for helpful discussions. This work was supported by NSF Grant No. DMR-9705131 (H.L.L.), and DMR-9120000 (G.B., M.V.K., and P.G.) through the STCS, and DOE-BES W-31-109-ENG-38 (D.G.H.).

REFERENCES

- [1] For a review, see S.L. Cooper and K.E. Gray, in *Physical Properties of High Temperature Superconductors IV*, edited by Donald M. Ginsberg (World Scientific, Singapore, 1994), p. 61, and references therein.
- [2] T. Ito *et al.*, *Nature* **350**, 596 (1991).
- [3] S. Tajima *et al.*, *Phys. Rev. B* **48**, 16164 (1993).
- [4] T. Timusk, D.N. Basov, and C.C. Homes, *J. Phys. Chem. Solids* **56**, 1821 (1995).
- [5] G. Kotliar *et al.*, *Europhys. Lett.* **15**, 655 (1991).
- [6] J.M. Wheatley, T.C. Hsu, and P.W. Anderson, *Nature* **333**, 121 (1988); *Phys. Rev. B* **37**, 5897 (1988); P.W. Anderson and Z. Zou, *Phys. Rev. Lett.* **60**, 132 (1988).
- [7] P.W. Anderson, *Physica C* **185**, 11 (1991); *Phys. Rev. Lett.* **67**, 660 (1991); *Science* **256**, 1526 (1992); S. Chakravarty *et al.*, *ibid.* **261**, 331 (1993); P.W. Anderson, *ibid.* **268**, 1154 (1995); *ibid.* **279**, 1196 (1998).
- [8] A.J. Leggett, *Science* **274**, 587 (1996); *ibid.* **279**, 1157 (1998).
- [9] S. Martin *et al.*, *Phys. Rev. Lett.* **60**, 2194 (1988); *Appl. Phys. Lett.* **54**, 72 (1989).
- [10] J.R. Cooper, L. Forro, and B. Keszzi, *Nature* **343**, 444 (1990).
- [11] T. Jacobs *et al.*, *Phys. Rev. Lett.* **75**, 4516 (1995); T. Shibauchi *et al.*, *Physica C* **264**, 227 (1996).
- [12] T.P. Devereaux and A.P. Kampf, *Int. J. Mod. Phys. B* **11**, 2093 (1997).
- [13] T. Staufer, R. Hackl, and P. Müller, *Solid State Commun.* **79**, 409 (1991); T. Staufer *et al.*, *Phys. Rev. Lett.* **68**, 1069 (1992); C. Kendziora and A. Rosenberg, *Phys. Rev. B* **52**, R9867 (1995); D. Einzel and R. Hackl, *J. of Raman Spectroscopy* **27**, 307 (1996); C. Kendziora, R.J. Kelley, and M. Onellion, *Phys. Rev. Lett.* **77**, 727 (1996); G. Blumberg

- et al.*, Science **278**, 1427 (1997), and references therein.
- [14] M. Boekholt, M. Hoffman, and G. Guentherodt, Physica C **175**, 127 (1991); O.V. Misochko and Gu Genda, *ibid.* **288**, 115 (1997).
- [15] D. Reznik *et al.*, Phys. Rev. B **46**, 11725 (1992); D. Reznik *et al.*, *ibid.* **48**, 7624 (1993); G. Blumberg *et al.*, *ibid.* **49**, 13295 (1994).
- [16] V.N. Denisov *et al.*, Solid State Commun. **70**, 885 (1989); M. Boekholt *et al.*, *ibid.* **74**, 1107 (1990).
- [17] Ran Liu *et al.*, Phys. Rev. B **45**, 7392 (1992).
- [18] M. Kakihana *et al.*, Phys. Rev. B **53**, 11796 (1996).
- [19] K.F. McCarty *et al.*, Phys. Rev. B **42**, 9973 (1990).
- [20] O.V. Misochko, K. Kuroda, and N. Koshizuka, Phys. Rev. B **56**, 9116 (1997).
- [21] T.P. Devereaux *et al.*, Phys. Rev. Lett. **72**, 396 (1994); T.P. Devereaux and D. Einzel, Phys. Rev. B **51**, 16336 (1995).
- [22] M.V. Klein and S.B. Dierker, Phys. Rev. B **29**, 4976 (1984).
- [23] W.E. Pickett, Rev. Mod. Phys. **61**, 433 (1989).
- [24] A.A. Abrikosov and V.M. Genkin, Sov. Phys.-JEPT **38**, 419 (1974).
- [25] H.L. Liu, *et al.* (unpublished).
- [26] S.L. Cooper *et al.*, Phys. Rev. Lett. **70**, 1533 (1993).
- [27] W.C. Wu and J.P. Carbotte, Phys. Rev. B **56**, 6327 (1997).
- [28] H. Kitano, T. Hanaguri, and A. Maeda, Phys. Rev. B **57**, 10946 (1998).
- [29] T. Shibauchi *et al.*, Physica C **203**, 315 (1992); S.-F. Lee *et al.*, Phys. Rev. Lett. **77**, 735 (1996).

[30] R. Kleiner *et al.*, Phys. Rev. Lett. **68**, 2394 (1992); R. Kleiner and P. Müller, Phys. Rev. B **49**, 1327 (1994); J-U. Lee *et al.*, Appl. Phys. Lett. **71**, 1412 (1997).

FIGURES

FIG. 1. Low-frequency Raman response functions in the zz polarization using red (1.92 eV) excitation. Thick line denotes the spectra taken at 5 K, and thin line at 100 K. The upper inset displays the difference between 5 K and 100 K spectra, using the procedure described in the text. The lower inset shows the sample faces that were used to measure Raman spectra.

FIG. 2. Raman spectra taken with six different polarizations at 5 K (thick line) and 100 K (thin line).

FIG. 3. Room-temperature c -polarized Raman scattering as a function of incident photon energy. The inset illustrates the normalized resonance Raman excitation profile of the zz (filled square) and xx (filled circle) continua compared with the imaginary part of the c -axis (solid line) and ab -plane dielectric constant (dotted line) [3,25].

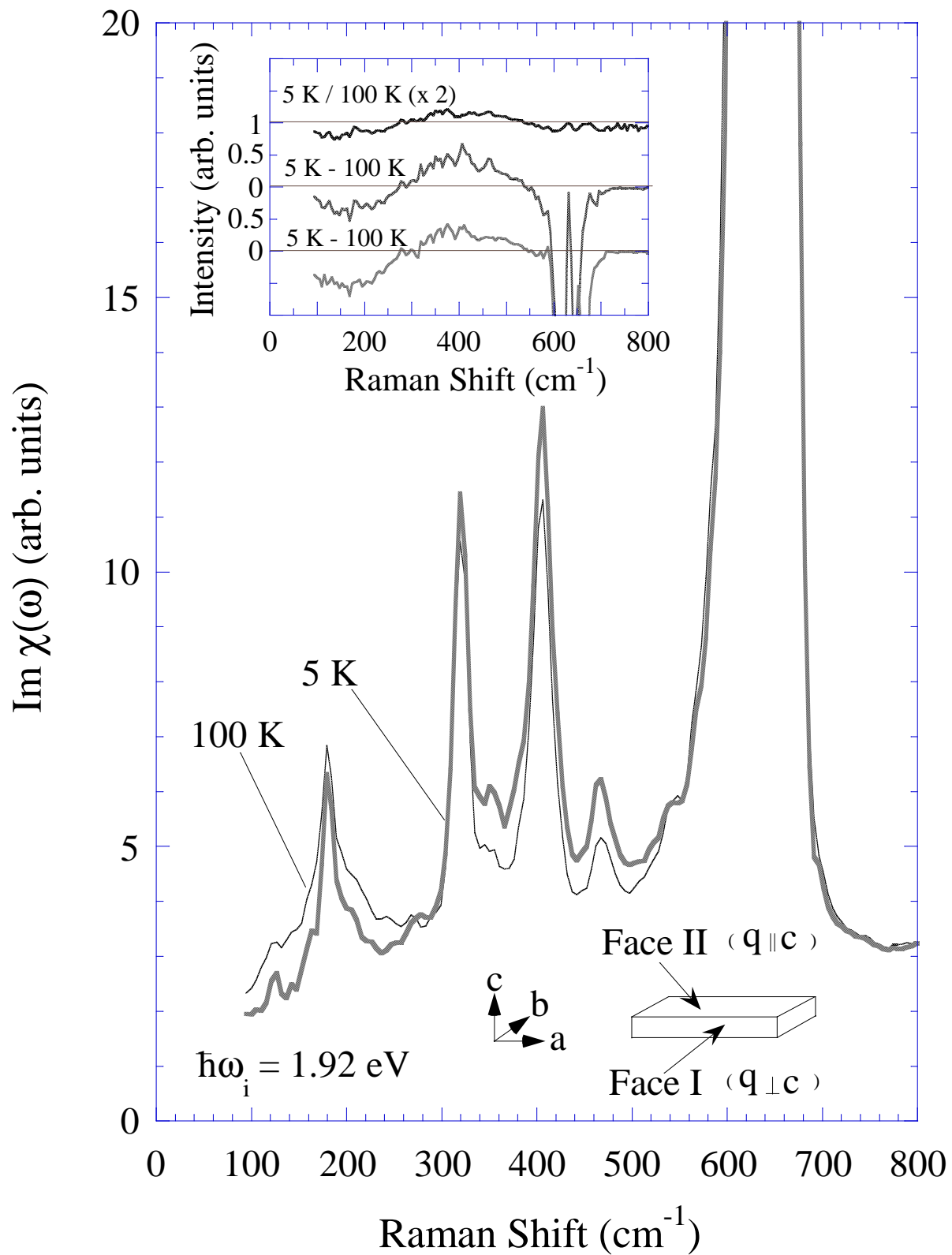


Fig. 1

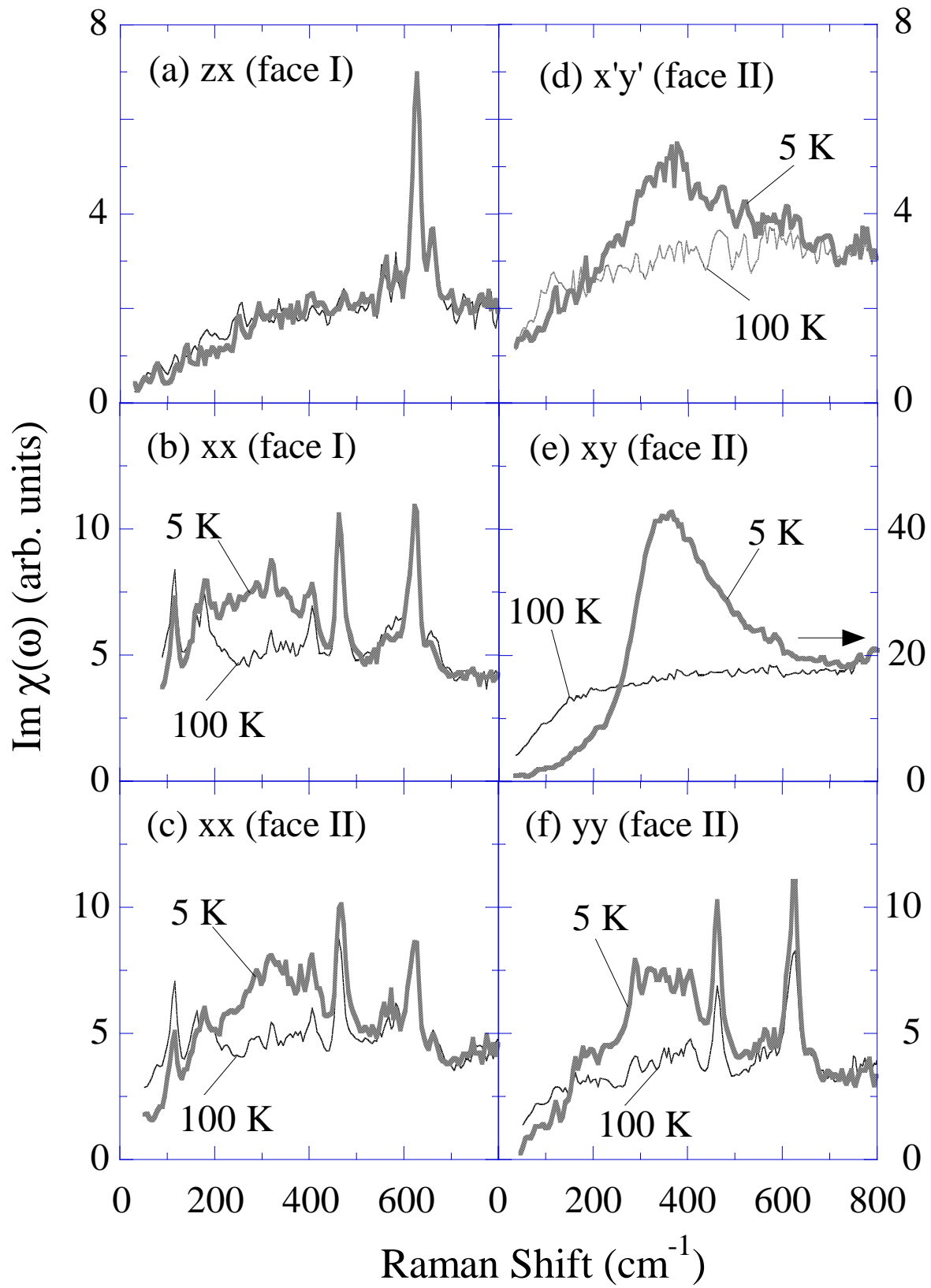


Fig. 2

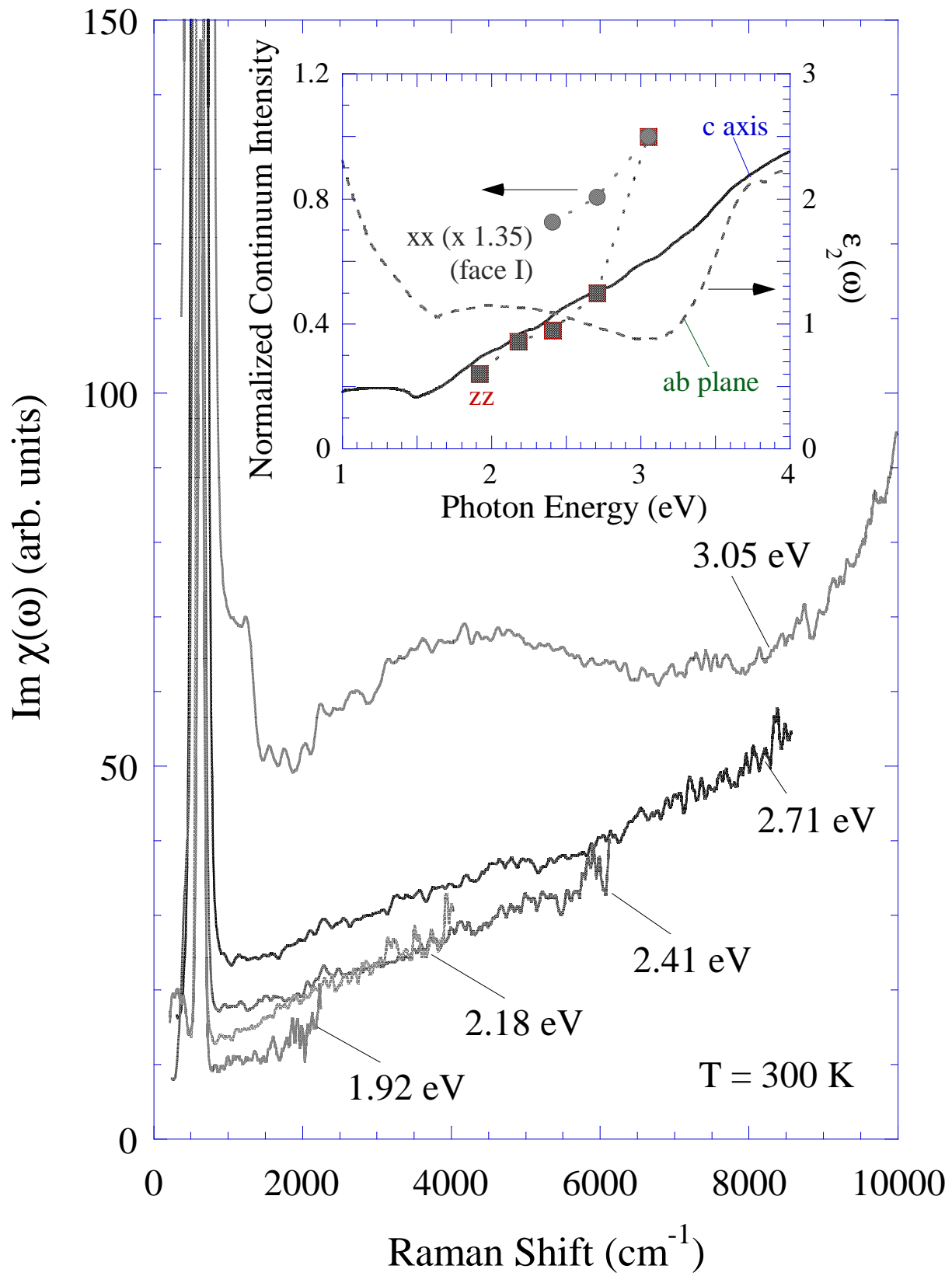


Fig. 3